Cranfield

College of Aeronautics Report No 9208
June 1992

RIEMANN SOLVERS FOR SOLVING THE INCOMPRESSIBLE NAVIER-STOKES EQUATIONS USING THE ARTIFICIAL COMPRESSIBILITY METHOD

D.T.Elsworth and E.F.Toro

College of Aeronautics
Cranfield Institute of Technology
Cranfield, Bedford MK43 0AL. England

Cranfield

College of Aeronautics Report No 9208
June 1992

RIEMANN SOLVERS FOR SOLVING THE INCOMPRESSIBLE NAVIER-STOKES EQUATIONS USING THE ARTIFICIAL COMPRESSIBILITY METHOD

D.T.Elsworth and E.F.Toro

College of Aeronautics
Cranfield Institute of Technology
Cranfield, Bedford MK43 0AL. England

ISBN 1 871564 549

£8.00

CRANFIELD
CoA Report 9208
June 1992

Riemann Solvers for Solving the Incompressible Navier-Stokes Equations using the Artificial Compressibility Method.

D.T.Elsworth and E.F.Toro
Departement of Aerospace Science
College of Aeronautics
Cranfield Institute of Technology
Cranfield, Beds MK43 0AL.

Riemann Solvers for Solving the Incompressible Navier-Stokes Equations using the Artificial Compressibility Method.

D.T.Elsworth and E.F.Toro
Department of Aerospace Science
College of Aeronautics
Cranfield Institute of Technology
Cranfield, Beds MK43 OAL

June 1992

1 Introduction.

The solution of the Incompressible Navier-Stokes equations still represents a significant numerical challenge. The reason for this is that there is a lack of a coupling between velocity and pressure. This means that the equations themselves provide no way of explicitly updating the pressure field as the velocity field is advanced. The artificial compressibility approach, devised by A.J.Chorin (see Chorin,1967), represents one way of overcoming this difficulty. It is arrived at by altering the incompressible equations in such a way as to result in a system of equations in which the left hand side is hyperbolic. We wish to take advantage of the hyperbolic nature of these equations and use Riemann-problem- based-numerical-methods (or RP methods).

Riemann-problem-based methods have long been used for the computation of inviscid, compressible, time dependent flows, and have more recently been extended for use with viscous, compressible flow regimes. For flows of these types, RP methods offer high shock resolution, with a large reduction in post shock oscillation when compared with traditional finite difference techniques with artificial viscosity. This is achieved by accurately representing the physical processes of shock propagation, adding the minimum amount of artificial diffusion needed to eliminate spurious oscillations, and applying this diffusion only where it is needed. Clearly those properties relating to numerical diffusion are advantageous for flow regimes where viscosity plays an important role in determining the flow solution. By adding only the minimum amount of artificial diffusion we can come closer to representing the true flow field.

Although RP based methods have these numerical advantages they also tend to be complicated and expensive. To a large extent this is due to the difficulties envolved in calculating the exact solution to the Riemann problem. However, the use of approximate solutions can significantly reduce the computational expense of this part of the numerical procedure. Since the flow solutions generated using the artificial compressibility equations are expected to be smooth we should be able to use approximate Riemann solvers without

any fear that they will fail due to overly large gradients in the flow. Five types of Riemann solver are presented in this report. The first of these is an exact, iterative solver, based on an the approach put forward by Toro (Toro, 1992). The second is based on a two rarefaction approximation which uses exact relations across rarefactions to to find the solution to the Riemann problem. The third is an approximate solver based on a local linearization proposed by Toro (Toro,1991). The fourth is a Roe type Riemann solver (Roe, 1981). Marx has already used a Roe Riemann solver in his work with the artificial compressibility method (Marx, 1991). The fifth Riemann solver is an extension of the HLL Riemann solver (Harten et.al., 1983), known as HLLC, in which the contact discontinuity is restored (Toro et.al, 1992). This is the first time that the author is aware of that an Exact solver for the artificial compressibility equations has been presented.

The remainder of this paper is organized as follows. In §2 the mathematical character of the artificial compressibility equations is introduced. §3 contains the exact Riemann solver, §4 deals with the Two Rarefaction Riemann solver, §5 contains the Local Linearization solver, §6 the Roe solver, and §7 the HLLC solver. All of these Riemann solvers are presented for the split two dimentional artificial compressibility equations in which viscosity has been neglected. The results of numerical tests perfomed on the various Riemann solvers are presented in §8, and conclusions are finally given in §9.

2 The Artificial Compressibility Equations.

As stated before, the artificial compressibility equations are a modification of the incompressible Navier-Stokes equations. However, for the time being, we will neglect the viscous terms, and use the inviscid artificial compressibility equations. These equations then form a set of hyperbolic conservation laws. In two dimensions the inviscid artificial compressibility equations are

$$\frac{\partial P}{\partial t} + \frac{\partial c^2 u}{\partial x} + \frac{\partial c^2 v}{\partial y} = 0 \tag{1}$$

$$\frac{\partial u}{\partial t} + \frac{\partial (u^2 + P)}{\partial x} + \frac{\partial vu}{\partial y} = 0 \tag{2}$$

$$\frac{\partial v}{\partial t} + \frac{\partial (v^2 + P)}{\partial y} + \frac{\partial uv}{\partial x} = 0 \tag{3}$$

P is pressure, u is x-direction velocity, v is the y-direction veloctiy and c is the artificial compressibility coefficient. We wish to find solutions to the split 2-D Riemann problem. The split two dimentional artificial compressibility equations can be written in matrix form as

$$\begin{bmatrix} P \\ u \\ v \end{bmatrix}_t + \begin{bmatrix} 0 & c^2 & 0 \\ 1 & 2u & 0 \\ 0 & v & u \end{bmatrix} \begin{bmatrix} P \\ u \\ v \end{bmatrix}_x = 0 \tag{4}$$

or

$$U_t + AU_x = 0 \tag{5}$$

Where A is the coefficient matrix, and U is the vector of conserved variables. The eigenvalues of the coefficient matrix A are

$$\lambda_1 = u - a, \lambda_2 = u, \lambda_3 = u + a, \tag{6}$$

where,

$$a = \sqrt{u^2 + c^2} \tag{7}$$

Thus we have three real, distict, eigenvalues and hence the system of equations is hyperbolic. The quantity a is analogous to the sound speed in the Euler equations, but here it depends on the velocity variable. The eigenvalues tell us that speed of the acoustic wave associated with the eigenvalue λ_1 is always negative, whilst speed of the acoustic wave associated with the eigenvalue λ_3 is always positive. The speed of the wave associated with the eigenvalue λ_2 lies between that of the other two waves. The eigenvalues have associated right eigenvectors

$$R_1 = \begin{bmatrix} -(a+u) \\ 1 \\ -v/a \end{bmatrix}, R_2 = \begin{bmatrix} 0 \\ 0 \\ 1 \end{bmatrix}, R_3 = \begin{bmatrix} (a-u) \\ 1 \\ v/a \end{bmatrix} \tag{8}$$

which can also be written as

$$R_1 = \begin{bmatrix} c^2 \\ (a-u) \\ \frac{-(u-a)v}{a} \end{bmatrix} R_2 = \begin{bmatrix} 0 \\ 0 \\ 1 \end{bmatrix}, R_3 = \begin{bmatrix} c^2 \\ (u+a) \\ \frac{(u+a)v}{a} \end{bmatrix}, \tag{9}$$

The Riemann Problem for the split two dimentional artificial compressibility equations consists of the initial value problem with piece-wise constant data P_L, u_L, v_L, and P_R, u_R, v_R. The left and right states (denoted by $_L$ and $_R$ respectively) are separated by a discontinuity at x=0. The solution to the Riemann problem entails four constant states separated by three waves, as shown in Figure 1. The waves associated with the eigenvalues $(u-a)$ and $(u+a)$ can be either rarefactions or shocks, depending on the initial conditions. Both the pressure and velocities change across these waves; in the the case of a shock the change is discontinuous, whilst for a rarefaction it is smooth. In the region between the waves, the so called *star region*, pressure and the x-direction velocity remain constant. Only the y-direction velocity changes across the contact discontinuity. The complete structure of the solution to Riemann problem is given in Figure 1.

3 Exact Solver.

The approach used here was orininally put forward by Toro (Toro, 1992). The main step in the solution strategy is to find the solution for u_*, the velocity in the star region. This is achived by finding an algebraic function of the form

$$F(u_*) = P_L - P_R + f_L(u_L, u_R) - f_R(u_L, u_R) = 0 \tag{10}$$

The form which the functions f_L and f_R take varies, and depends on the structure of the solution of the Riemann problem. We have two functions for each of the two waves; one for use when the wave is a rarefaction, and one for when it is a shock. The solution procedure is iterative, and at each iteration we need to decide on which combination of functions to use. Once u_* is known, P_* follows directly, as do v_{*L}, v_{*R}, and the wave speeds. If a rarefaction is present in the solution more work is required to find the distribution of pressure and velocity through the wave.

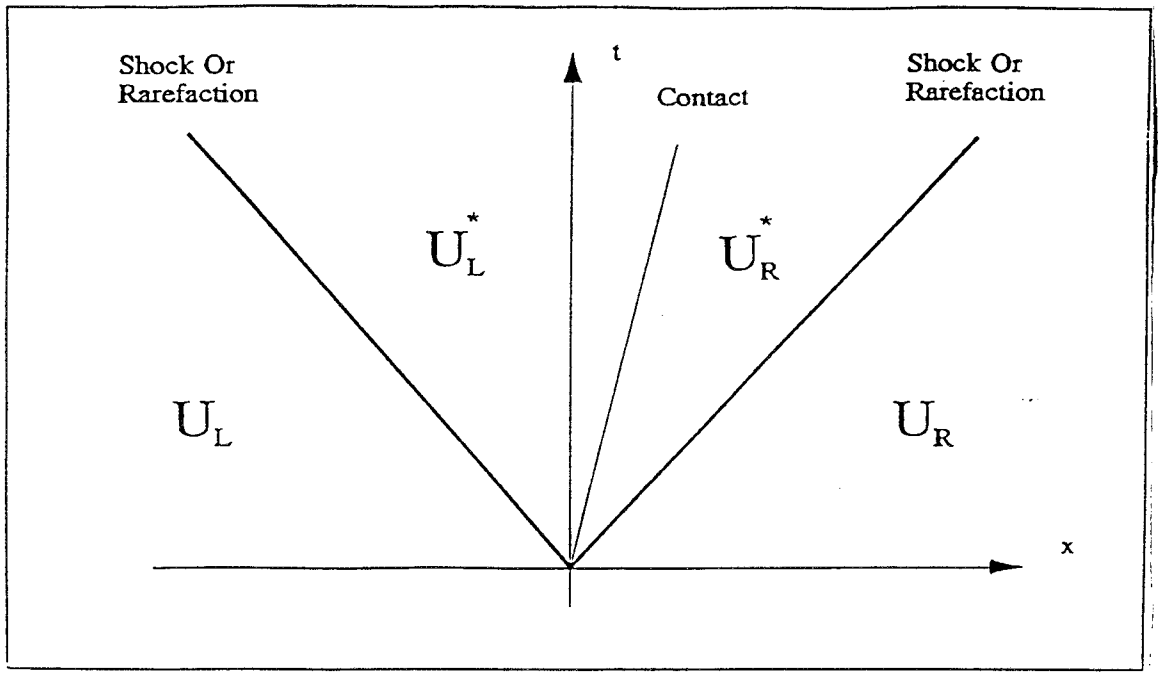

Figure 1: The Structure of the Riemann Poblem

Let us start by finding f_L and f_R, the functions for the relations across the left and right waves. We have four cases to consider.

CASE 1: The left wave is a rarefaction.

Here we apply the Riemann Invariants across the left wave. This is

$$\frac{dP}{-(a+u)} = du \tag{11}$$

and on integration this gives

$$P + \frac{c^2}{2}\left(\sinh^{-1}\left(\frac{u}{c}\right) + \frac{u\sqrt{u^2+c^2}}{c^2}\right) + \frac{u^2}{2} = CONSTANT \tag{12}$$

thus, when the left wave is a rarefaction, f_L is

$$\begin{aligned} f_L \;=\; & \frac{c^2}{2}\left(\sinh^{-1}\left(\frac{u_L}{c}\right) + \frac{u_L\sqrt{{u_L}^2+c^2}}{c^2}\right) + \frac{{u_L}^2}{2} \\ & -\frac{c^2}{2}\left(\sinh^{-1}\left(\frac{u_*}{c}\right) + \frac{u_*\sqrt{{u_*}^2+c^2}}{c^2}\right) - \frac{{u_*}^2}{2} \end{aligned} \tag{13}$$

CASE 2: The left wave is a shock.

Here we use the Rankine-Hugoniot jump conditions, ie,

$$S_L(P_* - P_L) = c_2(u_* - u_L) \tag{14}$$

and,

$$S_L(u_* - u_L) = (u_*{}^2 + P_*) - (u_L{}^2 + P_L) \tag{15}$$

Eliminating S, the shock speed, and rearranging we obtain a quadratic in $P_* - P_L$

$$\frac{(P_* - P_L)^2}{(u_* - u_L)} + (P_* - P_L)(u_* - u_L) - c^2(u_* - u_L) = 0 \tag{16}$$

which can be solved for $P_* - P_L$

$$P_* - P_L = \frac{-E \pm \sqrt{E^2 - 4DF}}{2D} \tag{17}$$

where

$$\begin{aligned} D &= \tfrac{1}{u_* - u_L} \\ E &= u_* + u_L \\ F &= -c^2(u_* - u_L) \end{aligned} \tag{18}$$

Now we need discover which sign to use. First we note that the presence of a *entropy satisfying* left shock requires that we have converging characteristics.

$$\lambda_1(u_L) = u_L - \sqrt{u_L{}^2 + c^2} > S > u_* - \sqrt{u_*{}^2 + c^2} = \lambda_1(u_*) \tag{19}$$

This gives $S < 0$ for all u_L,u_*. Now, we can examine the Rankine-Hugoniot condition. This tells us that if $(u_* - u_L) > 0$ then $(P_* - P_L) < 0$ and if $(u_* - u_L) < 0$ then $(P_* - P_L) > 0$. From equation (17) this means that the negative sign is the required one. Finally this gives

$$P_* - P_L = \frac{-E - \sqrt{E^2 - 4DF}}{2D} \tag{20}$$

CASE 3: The right wave is a rarefaction.

Following the same method as that used for the left rarefaction we can obtain.

$$\begin{aligned} f_R = &\frac{c^2}{2}\left(\sinh^{-1}\left(\frac{u_*}{c}\right) + \frac{u_*\sqrt{u_*{}^2 + c^2}}{c^2}\right) - \frac{u_*{}^2}{2} \\ &-\frac{c^2}{2}\left(\sinh^{-1}\left(\frac{u_R}{c}\right) + \frac{u_R\sqrt{u_R{}^2 + c^2}}{c^2}\right) + \frac{u_R{}^2}{2} \end{aligned} \tag{21}$$

CASE 4: The right wave is a shock.

Following the same method that was used for the left shock we utilize the Rankine-Hogoniot conditions

$$S_R(P_* - P_R) = c_2(u_* - u_R) \tag{22}$$

and,

$$S_R(u_* - u_R) = (u_*{}^2 + P_*) - (u_R{}^2 + P_R) \tag{23}$$

to obtain.

$$P_* - P_R = \frac{-E + \sqrt{E^2 - 4DF}}{2D} \tag{24}$$

where

$$\begin{aligned} D &= \tfrac{1}{u_*-u_R} \\ E &= u_* + u_R \\ F &= -c^2\,(u_* - u_R) \end{aligned} \tag{25}$$

Once again the the sign of the descriminant was found by ensuring that the shock is entropy satisfying, using the inequality

$$\lambda_3\,(u_R) = u_R + \sqrt{{u_R}^2 + c^2} > S > u_* + \sqrt{{u_*}^2 + c^2} = \lambda\,(u_*) \tag{26}$$

Notice that the sign of the descriminant differs from that in equation (20).

3.1 Solution Strategy.

The equation $F(u_*) = 0$ can be solved using Newton-Raphson iterative method. For this we require the derivatives of each function f_L, f_R. These are given below.

CASE 1: The left wave is a rarefaction.

The derivative of this function is;

$$f_L{}' = -\sqrt{{u_*}^2 + c^2} - u_* \tag{27}$$

CASE 2: The left wave is a shock.

The derivative of this function is;

$$f_L{}' = -\frac{1}{2}\left[(u_L + u_*) + Q + (u_L - u_*)\left(1 + \frac{(u_* + u_L)}{Q}\right)\right] \tag{28}$$

where

$$Q = \sqrt{(u_* + u_L)^2 + 4c^2} \tag{29}$$

CASE 3: The right wave is a rarefaction.

The derivative of this function is;

$$f_R{}' = +\sqrt{{u_*}^2 + c^2} - u_* \tag{30}$$

CASE 4: The right wave is a shock.

The derivative of this function is;

$$f_R{}' = -\frac{1}{2}\left[(u_R + u_*) + Q + (u_* - u_R)\left(1 + \frac{(u_* + u_R)}{Q}\right)\right] \tag{31}$$

where

$$Q = \sqrt{(u_* + u_R)^2 + 4c^2} \tag{32}$$

3.2 The Solution for Pressure.

Once u is known through the star region, the pressure can be determined from the functions governing relations across waves that we have already found. The function used depends on the wave structure present and whether the the function for left or the right wave is being used. For example, if we are using the expression for the left wave, the pressure in the star region is

$$P_* = P_L + f_L \tag{33}$$

Which f_L we use depends on whether the left wave is a rarefaction or a shock.

3.3 The Solution for y-Direction Velocity.

The final step in finding the solution in the star region is to find the y-direction velocity. The y-direction velocity changes across the left and right acoustic waves, as well as across the central contact wave. In this way it is analogous to density in the Euler equations. Once again, the way in which the solution is determined depends on the types of waves that are present.

CASE 1: The left wave is a rarefaction.

In this case we again deploy Riemann invariants. For the left wave these give

$$du = -\frac{v}{a}dv \tag{34}$$

which on integration and subsequent manipulation provides

$$v_{*L} = v_L \exp\left(sinh^{-1}\left(u_L/a_L\right) - sinh^{-1}\left(u_*/a_*\right)\right) \tag{35}$$

where

$$a_L = \sqrt{u_L^2 + c^2}, a_* = \sqrt{u_*^2 + c^2} \tag{36}$$

CASE 2: The left wave is a shock.

In this case the Rankine-Hugoniot jump conditions are used

$$S_L\left(v_{*L} - v_L\right) = \left(u_* v_{*L} - u_L v_L\right) \tag{37}$$

which gives

$$v_{*L} = v_L\left(\frac{1 - u_L/S_L}{1 - u_*/S_L}\right) \tag{38}$$

where S_L is the speed of the shock. This can be found from equation (14).

CASE 3: The right wave is a rarefaction.

Again we use the Riemann invariants, and obtain

$$v_{*R} = v_R \exp\left(sinh^{-1}\left(u_*/a_*\right) - sinh^{-1}\left(u_R/a_R\right)\right) \tag{39}$$

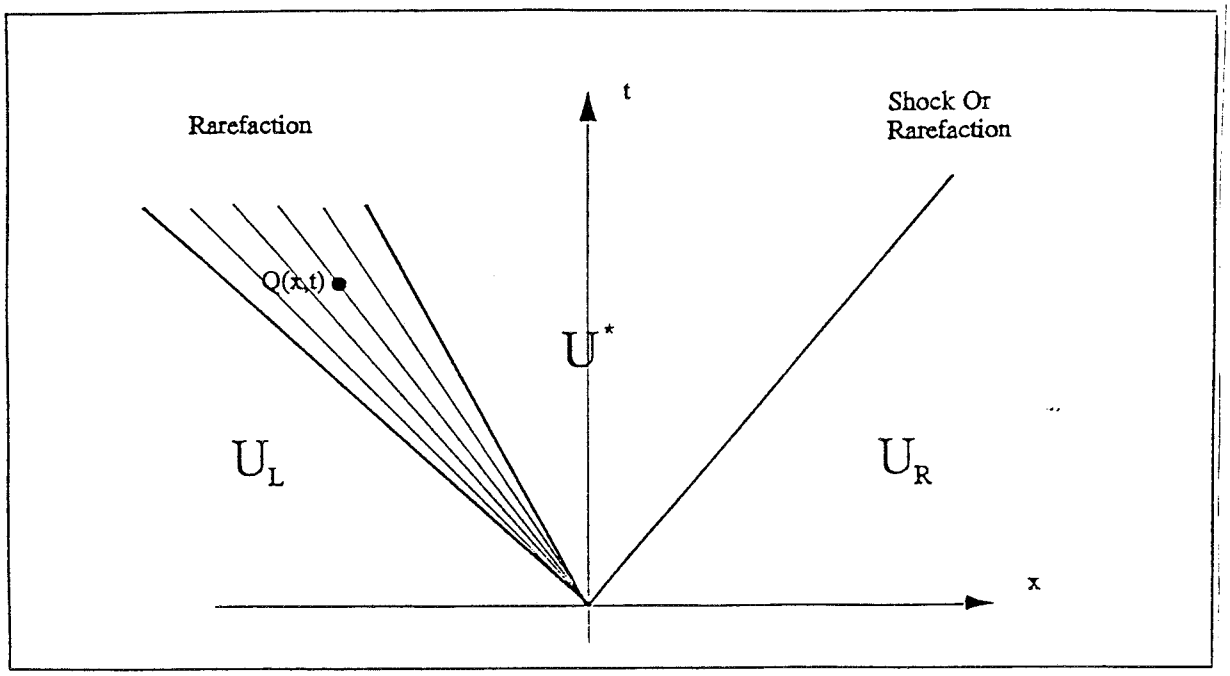

Figure 2: The Solution Within a Rarefaction

CASE 4: The right wave is a shock.

Using the Rankine-Hugoniot jump conditions we can obtain

$$v_{*R} = v_L \left(\frac{1 - u_R/S_R}{1 - u_*/S_R} \right) \tag{40}$$

where S_R is the speed of the shock. This can be found from equation 22.

3.4 The Solution Within a Rarefaction.

When one or more of the waves in the solution to the Riemann problem are rarefactions it is necessary to find the value of u,P, and v within the wave, since these vary smoothly within the rarefaction. Consider the case of the left rarefaction wave. We wish to find the value of u at the point $Q(x,t)$ within the wave as shown in Figure 2. The equation of the characteristic that passes through $(0,0)$ and (x,t) is

$$\frac{dx}{dt} = u - \sqrt{u^2 + c^2} = \frac{x}{t} \tag{41}$$

and has constant slope, so u is simply the solution of the equation.

$$u - \sqrt{u^2 + c^2} - \frac{x}{t} = 0 \tag{42}$$

Likewise for the right wave u is the solution of the equation

$$u + \sqrt{u^2 + c^2} - \frac{x}{t} = 0 \tag{43}$$

Both of these can be solved using Newton-Raphson.

The solution for pressure within a rarefaction can be found using the expression linking variables across rarefactions since the Riemann invariants hold across any and all of the waves within the rarefaction. Thus the solution within a left moving rarefaction would be

$$\begin{aligned} P &= P_L + \frac{c^2}{2}\left(\sinh^{-1}\left(\frac{u_L}{c}\right) + \frac{u_L\sqrt{{u_L}^2+c^2}}{c^2}\right) + \frac{{u_L}^2}{2} \\ &\quad -\frac{c^2}{2}\left(\sinh^{-1}\left(\frac{u}{c}\right) + \frac{u\sqrt{u^2+c^2}}{c^2}\right) - \frac{u^2}{2} \end{aligned} \tag{44}$$

and within the right moving rarefaction

$$\begin{aligned} P &= P_R - \frac{c^2}{2}\left(\sinh^{-1}\left(\frac{u_R}{c}\right) + \frac{u_R\sqrt{{u_R}^2+c^2}}{c^2}\right) + \frac{{u_R}^2}{2} \\ &\quad +\frac{c^2}{2}\left(\sinh^{-1}\left(\frac{u}{c}\right) + \frac{u\sqrt{u^2+c^2}}{c^2}\right) - \frac{u^2}{2} \end{aligned} \tag{45}$$

Finally we need to find an expressions for the y-direction velocity within rarefactions within a left moving rarefaction we have

$$v = v_L \exp\left(sinh^{-1}\left(u_L/a_L\right) - sinh^{-1}\left(u/a\right)\right) \tag{46}$$

where

$$a_L = \sqrt{u_L^2 + c^2}, a = \sqrt{u^2 + c^2} \tag{47}$$

and for a right moving rarefaction

$$v_{*R} = v_R \exp\left(sinh^{-1}\left(u/a\right) - sinh^{-1}\left(u_R/a_R\right)\right) \tag{48}$$

where

$$a_R = \sqrt{u_R^2 + c^2}, a = \sqrt{u^2 + c^2} \tag{49}$$

3.5 Wave Speeds.

Once the values of velocity and pressure in the star region are known, and the solution through any rarefactions has been determined, all that remains is for the wave speeds to be determined. These are given below.

CASE 1: The left wave is a rarefaction.

A rarefaction has two significant wave speeds, that associated with the head, and that associated with the tail. These speeds can be found using the eigenvalues for the states on either side of the rarefaction.

$$S = u - \sqrt{u^2 + c^2} \tag{50}$$

CASE 2: The left wave is a shock.

Again we use the Rankine-Hogoniot conditions. The simplest of these to evaluate is

$$S_L(P_* - P_L) = c^2(u_* - u_L) \tag{51}$$

giving

$$S_L = c^2 \frac{(u_* - u_L)}{(P_* - P_L)} \tag{52}$$

CASE 3: The right wave is a rarefaction.

For a right rarefaction speeds we use the eigenvalue

$$S = u + \sqrt{u^2 + c^2} \tag{53}$$

for the states on either side of the rarefaction.

CASE 4: The right wave is a shock.

Using the Rankine-Hogoniot condition we have

$$S_R = c^2 \frac{(u_* - u_R)}{(P_* - P_R)} \tag{54}$$

4 Two Rarefaction Solver.

The Two Rarefaction Riemann solver is based, not suprisingly, on the assumption or approximation that both of the acoustic waves are rarefactions. The exact relations across rarefactions are then used to find the solution in the star region. For some sets of equations this approach results in a closed system for which the solution in the star region can be found directly. This is not the case for the artificial compressibility equations, and as with the exact Riemann solver an iterative technique is required. The algebraic function that is solved to find u_* is,

$$F(u_*) = P_L - P_R + f_L(u_L, u_R) - f_R(u_L, u_R) = 0 \tag{55}$$

f_L and f_R are given by equations (13) and (22), the functions giving the relationships of variables across rarefactions. Pressure in the star region can be found using equations (33) and (13), and the y-direction velocities using equation (35) and equation (39).

5 Local Linearization Solver.

Here we present a split two dimensional linearized Riemann solver. It follows the approach used by E.F. Toro for the Euler equations (Toro, 1991a). The basis of this approach is to seek a solution to the Riemann problem for a local linearization of the equations. We assume that, if the left and right states are sufficiently close to each other, the coefficient matrix $[A]$ is constant for a given Riemann problem. Further more, we assume that A can

be expressed in terms of an average state. This average state is expressed in terms of the left and right states, and a linear system is produced.

$$U_t + \bar{A}U_x = 0 \tag{56}$$

where

$$\bar{A} = \begin{bmatrix} 0 & c^2 \\ 1 & 2\bar{u} \end{bmatrix} \tag{57}$$

and $\bar{u}$ is a local average velocity, yet to be defined. Note that $\bar{u}$ implies a local wave speed

$$\bar{S} = \bar{u} \pm \bar{a} \tag{58}$$

where

$$\bar{a} = \sqrt{\bar{u}^2 + c^2} \tag{59}$$

Having perfomed this linearization we can now use standard tequniques for linear hyperbolic systems. We apply Riemann invariants across the waves of the approximate system. Using the eigenvectors given in equation (8) for the left wave gives

$$\frac{dP}{c^2} = \frac{du}{\bar{u} - \bar{a}} \tag{60}$$

which on integration produces

$$P_L - \frac{c^2}{\bar{u}^2 - c^2} u_L = P_* - \frac{c^2}{\bar{u}^2 - c^2} u_* \tag{61}$$

Doing the same for the right wave we obtain

$$\frac{dP}{c^2} = \frac{du}{\bar{u} + \bar{a}} \tag{62}$$

and

$$P_R - \frac{c^2}{\bar{u}^2 + c^2} u_R = P_* - \frac{c^2}{\bar{u}^2 + c^2} u_* \tag{63}$$

Combining equations (61) and (63) to eliminate u_* we have an expression for the pressure in the star region.

$$P_* = \frac{c^2}{2\bar{a}} (u_L - u_R) + \frac{\bar{u}}{2\bar{a}} (P_R - P_L) + \frac{1}{2} (P_R + P_L) \tag{64}$$

Using the alternative eigenvectors given in equation (9) we can again use the Riemann invariants to give

$$P_L + (\bar{u} - \bar{a}) u_L = P_* + (\bar{u} - \bar{a}) u_* \tag{65}$$

and

$$P_R + (\bar{u} + \bar{a}) u_R = P_* + (\bar{u} + \bar{a}) u_* \tag{66}$$

from which we can obtain

$$u_* = \frac{1}{2\bar{a}} (P_L - P_R) \frac{\bar{u}}{2\bar{a}} (u_L - u_R) + \frac{1}{2} (u_L + u_R) \tag{67}$$

Thus we can find u_* and P_* and all that remains is to find v_{*L} and v_{*R}. This can be acived using the left and right Riemann invariants. First, the left wave

$$du = -\frac{\bar{v}}{\bar{a}}dv \tag{68}$$

giving

$$v_{*L} = \frac{(u_L - u_*)\,\bar{v}}{\bar{a}} + v_L \tag{69}$$

Using a similar approach for the right wave we get

$$v_{*R} = \frac{(u_* - u_R)\,\bar{v}}{\bar{a}} + v_R \tag{70}$$

6 Roe Solver.

The Roe approach to approximately solving the Riemann problem (Roe, 1981) is similar in philosophy to that of the local linearization solver. Again we are seeking a linear approximation to the coefficient matrix A. Now, however, we wish to construct a matrix that will satisfy specific conditions. Roe suggested these conditions in his paper, and showed how to satisfy them and find an approximate solver. Here we follow one methodology. For a linear system we known that the data difference can be decomposed in terms of the right eigenvectors $\overline{R_k}$, and the wave strengths $\overline{\alpha_k}$ as

$$\Delta U = \sum_{k=1}^{n} \overline{\alpha_K R_k} \tag{71}$$

When this is applied to the artificial compressibility equations it gives

$$\Delta P = \overline{\alpha_1}c^2 + \overline{\alpha_3}c^2 \tag{72}$$

$$\Delta u = \overline{\alpha_1}(\overline{u} - \overline{a}) + \overline{\alpha_3}(\overline{u} + \overline{a}) \tag{73}$$

$$\Delta v = -\overline{\alpha_1}\frac{(\overline{u} - \overline{a})\,\overline{v}}{\overline{a}} + \overline{\alpha_2} + \overline{\alpha_3}\frac{(\overline{u} + \overline{a})\,\overline{v}}{\overline{a}} \tag{74}$$

The overbar represents quantities that are evaluated in terms of some average value yet to be found. Equation (73) gives

$$\overline{\alpha_1} = \frac{\Delta P - \overline{\alpha_3}c^2}{c^2} \tag{75}$$

$$\overline{\alpha_3} = \frac{\Delta P - \overline{\alpha_1}c^2}{c^2} \tag{76}$$

Substituting equation (76) into equation (74) gives

$$\alpha_1 = \frac{\Delta P}{2\overline{a}c^2}(\overline{u} + \overline{a}) - \frac{\Delta u}{2\overline{a}} \tag{77}$$

Similarly substituting equation (76) into equation (74) gives

$$\alpha_3 = \frac{\Delta u}{2\overline{a}} - \frac{\Delta P}{2\overline{a}c^2}(\overline{u} + \overline{a}) \tag{78}$$

Another expression that is valid for linear systems is

$$\Delta F = \sum_{k=1}^{2} \overline{\alpha_k \lambda_k R_k} \tag{79}$$

or

$$c^2 \Delta u = \overline{\alpha_1} c^2 (\overline{u} - \overline{a}) + \overline{\alpha_3} c^2 (\overline{u} + \overline{a}) \tag{80}$$

$$\Delta u^2 + \Delta P = \overline{\alpha_1} (\overline{u} - \overline{a})^2 + \overline{\alpha_3} (\overline{u} + \overline{a})^2 \tag{81}$$

It can be seen that equation (81) is the same as equation (74), so we have three equations and three unknowns. Now we substitute equations (77) and (78) into equation (81), which gives

$$\overline{u} = \frac{\Delta u^2}{2 \Delta u} \tag{82}$$

and since

$$\Delta u^2 = u_R^2 - u_L^2 \tag{83}$$

$$\Delta u = u_R - u_L \tag{84}$$

we obtain

$$\overline{u} = \frac{1}{2} (u_R + u_L) \tag{85}$$

In its original form the definition of the Roe intercell flux used was

$$F(U_L, U_R) = \frac{1}{2} (F(U_L) + F(U_R)) - \frac{1}{2} \sum_{k=1}^{2} |\overline{\lambda_k}| \, \overline{\alpha_k R_k} \tag{86}$$

However it is posible to re-interpret Roe's method to give the conserved variables in the star region and this is the approach adopted here. For details of this see (Toro,1991b).

7 HLLC Solver.

The HLLC solver is an extension of the Harten-Leer-Lax Riemann solver (Harten et.al, 1983), in which the contact discontinuity is re-introduced into the solution. The 'C' in HLLC stands for contact. The first step of in this approach is to find estimates of wave speeds. Note that for the HLLC Riemann solver this includes finding a wave speed for the contact, and this depends on the solution to the Riemann problem. There is any number of ways in which the wave speeds can be found, but one reliable method is to use the linearised solver, as we have done here. This provides us with u_*, and we need to find the rest of the vector of conserved variables. When used in its pure form, the HLLC method provides us with P_{*L},P_{*R},v_{*L}, and v_{*R}. This is at odds with the known exact solution in which pressure is constant within the star region, and so it may be advisable to use other sources for providing the pressure in the star region. For example, one could average the values of P_{*L} and P_{*R}, or use HLL to calculate P_*, as we have done here. Then all that remains is to find v_{*L} and v_{*R}. The first of these is found using

$$S_L v_{*L} - u_* v_{*L} = S_L v_L - u_L v_L = q_L \tag{87}$$

For an explanation of the source of this relationship see (Toro et.al, 1992). This then gives

$$v_{*L} = \frac{q_L}{S_L - u_*} \tag{88}$$

For the right star y-direction velocity we use

$$S_R v_{*R} - u_* v_{*R} = S_R v_R - u_R v_R = q_R \tag{89}$$

which gives

$$v_{*R} = \frac{q_R}{S_R - u_*} \tag{90}$$

Finally the vectors of conserved variables in the star region are used to compute the star fluxes using

$$F_{*L} = F_L + S_L(U_{*L} - U_L) \tag{91}$$

$$F_{*R} = F_R + S_R(U_{*R} - U_R) \tag{92}$$

8 Numerical Results.

Two types of test case are presented here. Firstly we compare the results obtained for the values of pressure and velocity in the star region for a single Riemann problem. The approximate solvers are compared with the exact Riemann solver. Next the solutions obtained from a FORTRAN program which was written to solve the one dimensional artificial compressibility equations are compared. The program uses the first order Godunov method in conjunction with the solvers presented, which are used to solve the local Riemann problems. In addition to assesing the accuracy of the solutions generated consideration is given to the robustness and computational expense of each Riemann solver. The test Riemann problem used for all of these tests is shown in Table 1. This test problem is a harsh one, especially in the context of the artificial compressibility equations, where smooth flow solutions are to be expected. However, it is desirable to use such a test in order to get an idea of the robustness of the approximate solvers. The results for the first test are given in Table 2. This shows the fluxes in the star region. The reason that the fluxes, and not the conserved variables, are given is two-fold. Firstly, it is the fluxes that are used to update the variables in RP based methods, and secondly, the HLLC Riemann solver gives the fluxes, not the conserved variables. These results show several interesting features. The Roe type solver, and the linear solver give identical results. This is not particularly surprising, given that they are based on the same average state, namely $\overline{U} = \frac{1}{2}U$. In fact it is a simple task to verify that the two methods are identical for this case. It is also notable that the Roe and Linear solvers are the least accurate of the solvers for this test case. The results obtained for the two rarefaction Riemann solver are much better that those obtained by the other solvers. Having said all of this, it has to be remembered that this test case is much harsher that we would expect to meet when solving the equations to find the solution to the Navier-Stokes equations.

Figures 3 to 7 show the results obtained using the different Riemann solvers to solve a global Riemann problem using the Godunov method. They were performed at a CFL coefficient of 0.9, with 100 computational cells, and the artificial compressibility coefficient,

c, was set at 0.9. The results are given for a time of 0.1. As a whole, they point out one of the strenghts of Riemann-Problem-based methods. Although some of the approximate Riemann solvers are quite inaccurate locally, the quality of the results is good. This is due to two factors; firstly, it is the flux difference that is used to update the conserved variables, and secondly, RP based methods ensure conservation. These results are very reassuring, and any of the approximate Riemann solvers can safely be used. This is bourn out by the results given in Table 3. This shows a sum of the differences between the results obtain using the exact solver and the approximate solvers, ie.

$$E = \frac{1}{N} \sum_{i=1}^{N} \sqrt{e_i^2}$$

where

$$e_i = |U_i^{approx} - U_i^{exact}|$$

This shows that there are no large discrepancies between the solutions generated using the the exact solver and those generated with the approximate solvers.

The final test performed was to compare the efficiency of the Riemann solvers. The CPU time taken for the above test problem, with 1000 cells, was measured and these are shown in Table 4. The linear solver is the least computationally expensive of the solvers, the two rarefaction approximation solver is the most expensive. At first glance it is surprising that the two rarefaction solver is more expensive than the exact solver. After all it is suposed to be a simplification. On closer analysis this phenomenon does make sence. In the two rarefaction approximation we are itteratively solving the wrong exact expressions, so that it may take longer for the solution to converge. In addition to this the expressions for a rarefaction are more complicated than those for a shock. The HLLC solver lies in the middle of the range of Riemann solvers, and to a large extent the computational expense comes from finding reliable estimates for the wave speeds. In the above example this is done using the linear solver, and so the HLLC solver must take at least as long as the linear solver.

9 Conclusion

Five Riemann solvers for the artificial compressibility equations have been presented. All of these give accurate results when used to produce global solutions to the test problem. Although this may not be the case for more demanding cases, test problem given is harsher than what we would expect to find in a solution to the Navier-Stokes equations. The two rarefaction solver is computationally expensive, and offers no special advantage over the other solvers and so is not a good choice. The linear solver is the cheapest computationally, is simple and has proven sufficiently accurate to use in a program to find the solution to the Navier-Stokes equations. The HLLC solver is also relatively cheap, and has a reputation for being very robust. Under certain conditions it may be better to select this solver above the linear one.

u_L	1.0
v_L	1.0
P_L	0.1
u_R	1.0
v_R	0.5
P_R	1.0

Table 1: The Test Case.

Solver	$c^2 u_*$		$u_* v_{*L}$		$u_* v_{*R}$		$u_*^2 + P_*$	
	Output	%	Output	%	Output	%	Output	%
Exact	0.51010	0.0	0.85635	0.0	0.23202	0.0	1.2478	0.0
Two Rare'	0.51045	0.069	0.85480	0.169	0.23200	0.008	1.2486	0.064
Roe	0.53907	5.679	0.78961	7.794	0.20866	10.07	1.3274	6.379
Linear	0.53907	5.679	0.78961	7.794	0.20866	10.07	1.3274	6.379
HLLC	0.46778	8.296	0.86439	0.939	0.26650	14.86	1.2155	2.589

Table 2: Comparison of Results for Local Riemann Problem.

Solver	u	v	P
Exact	0.0	0.0	0.0
Two Rare'	5.2508×10^{-7}	3.3184×10^{-7}	1.8900×10^{-7}
Roe	2.7507×10^{-5}	1.7918×10^{-4}	3.1680×10^{-5}
Linear	2.7507×10^{-5}	1.7918×10^{-4}	3.1680×10^{-5}
HLLC	1.3050×10^{-4}	9.4740×10^{-5}	5.6512×10^{-4}

Table 3: Summation of errors.

Solver	CPU Units
Exact	269.9
Two Rare'	283.4
Roe	66.5
Linear	60.7
HLLC	106.7

Table 4: CPU Units in seconds.

10 References

Marx, Y.P. 1991. Evaluation of the Artificial Compressibility Method for the Solution of the Incompressible Navier-Stokes Equations. 9th GAMM Conference of Numerical Methods in Fluid Mechanics. Lausanne, Sept. 1991.

Rizzi, A., Erikson L. 1985. Computation of Inviscid Incompressible Flow with Rotation. Journal of Fluid Mechanics. vol 153, pp 275-312.

Roe, P.L. 1981. Approximate Riemann Solvers, Parameter Vectors, and Difference Schemes. Journal of Computational Physics. 43: 357-365.

Harten, A., Lax, P., van Leer, D. 1983. On Upstream Differencing and Godunov-type Methods for Hyperbolic Conservation Lews. SIAM Review 25, 35-61.

Toro, E.F. 1991a. A Linearized Riemann Solver for the Time-Dependent Euler Equations of Gas Dynamics. Proc. R. Soc. Lond. A(1991) 683-693.

Toro, E.F. 1991b. The Weighted Average Flux Method Applied to the Euler Equations. (In Press).

Toro, E.F. 1992. Riemann Problems and the WAF Method for the Two-Dimensional Shallow Water Equations.Phil. Trans Roy. Soc. London. A (1992) 338, 43-68.

Toro, E.F., Spuce, M., Spears, W. 1992. Restoration of the Contact Surface in the HLL Riemann Solver. (Submitted).

Exact Solver.

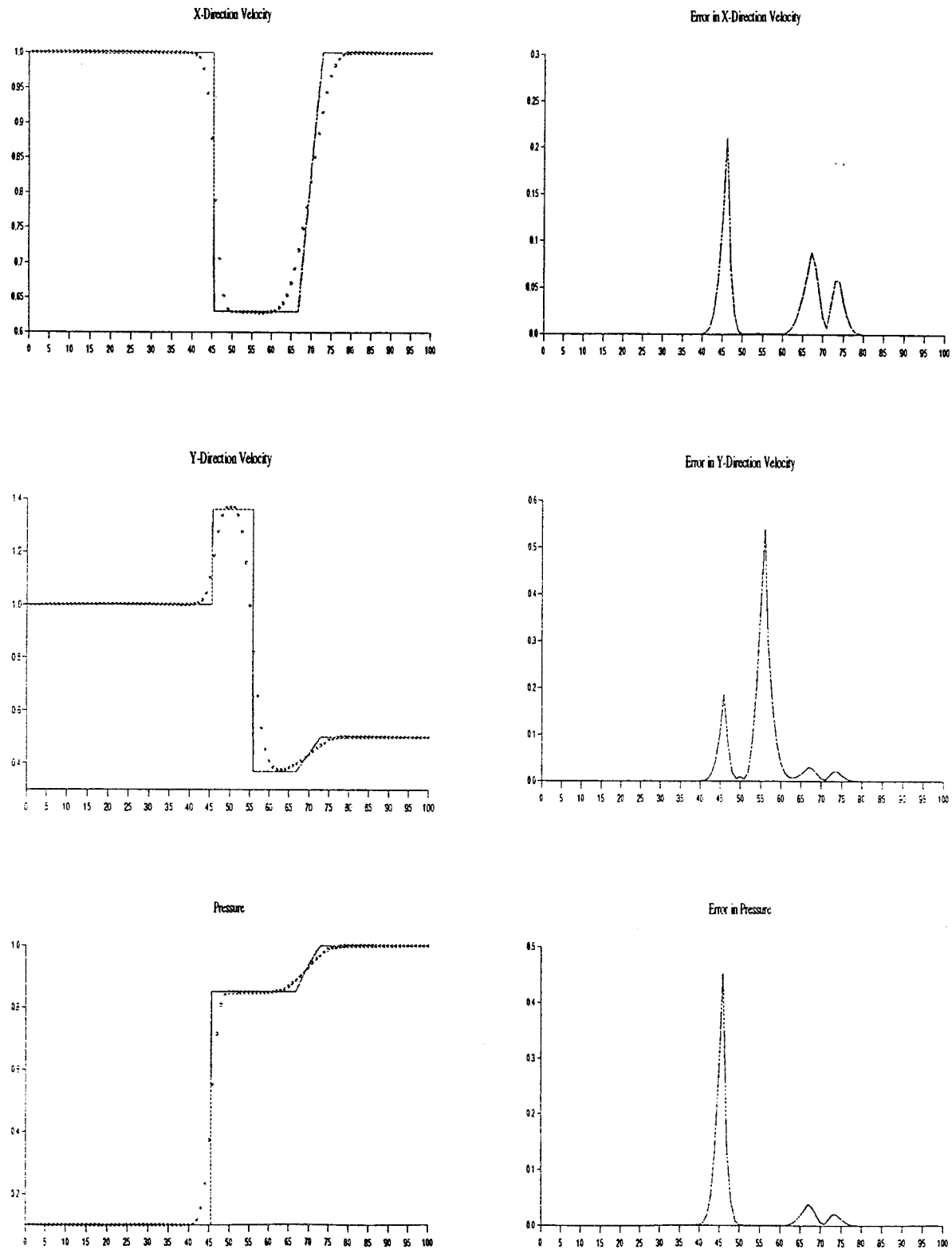

Figure 3: Exact Riemann Solver

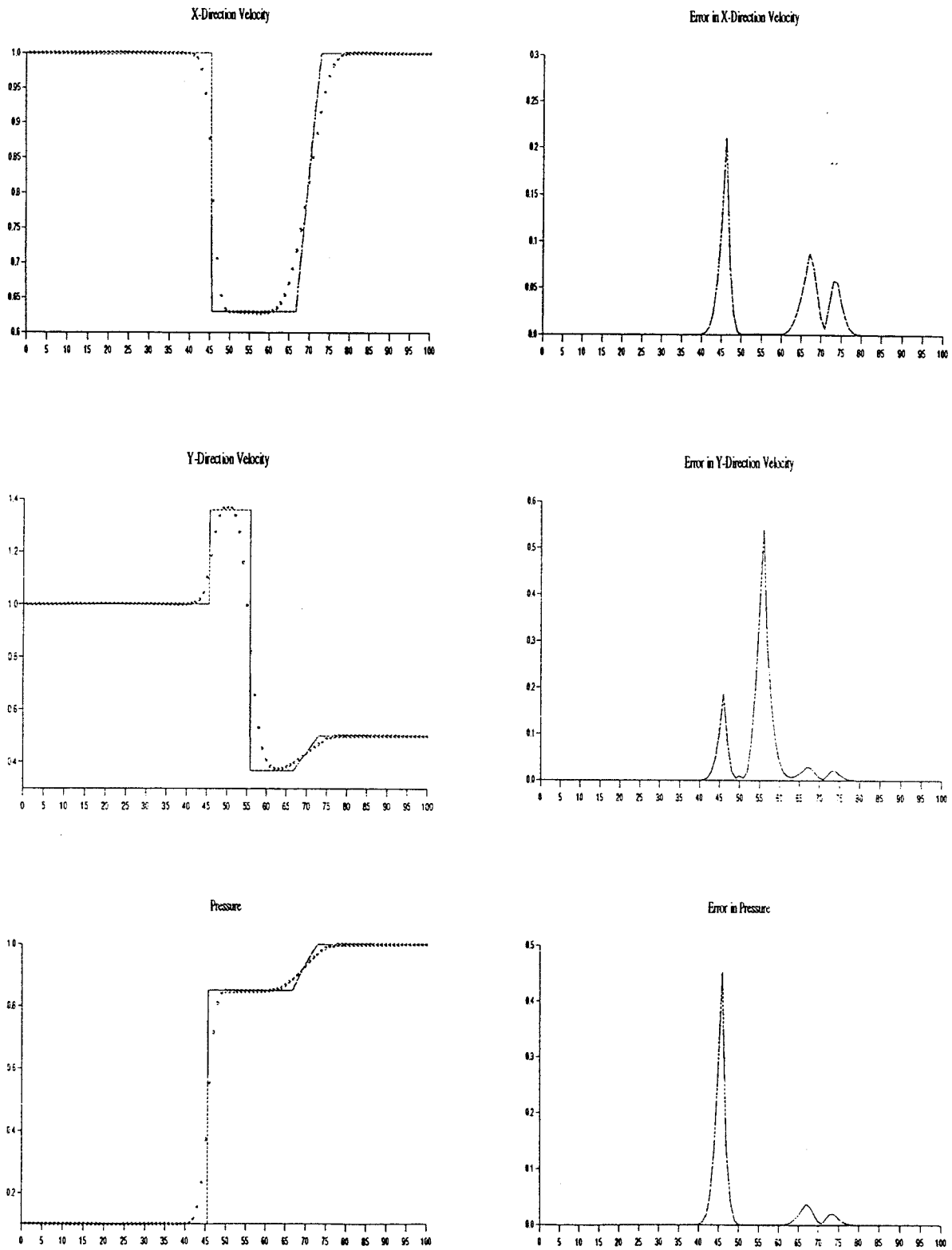

Figure 4: Two Rarefaction Riemann Solver

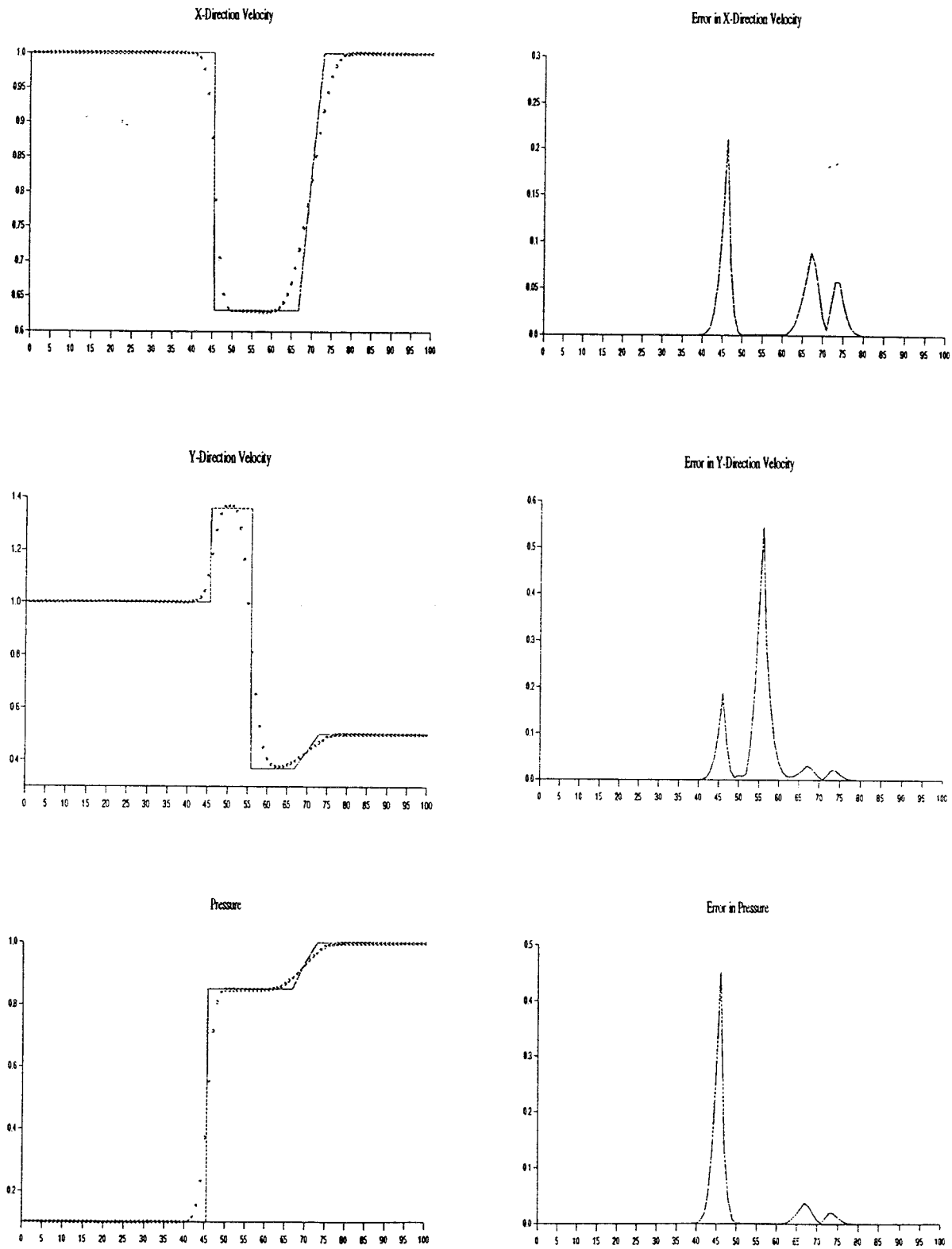

Figure 5: Roe Riemann Solver

Linear Solver.

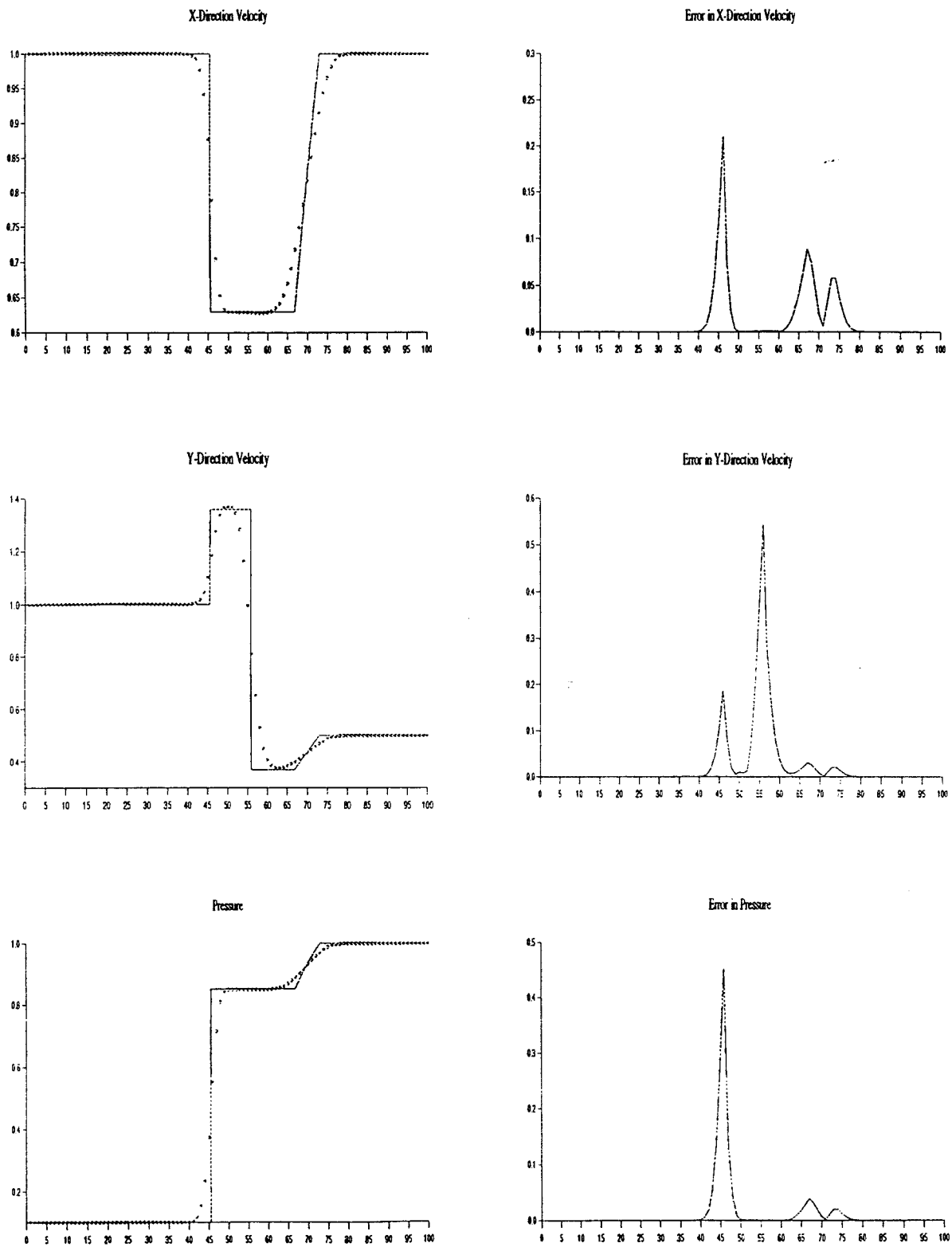

Figure 6: Linearized Riemann Solver

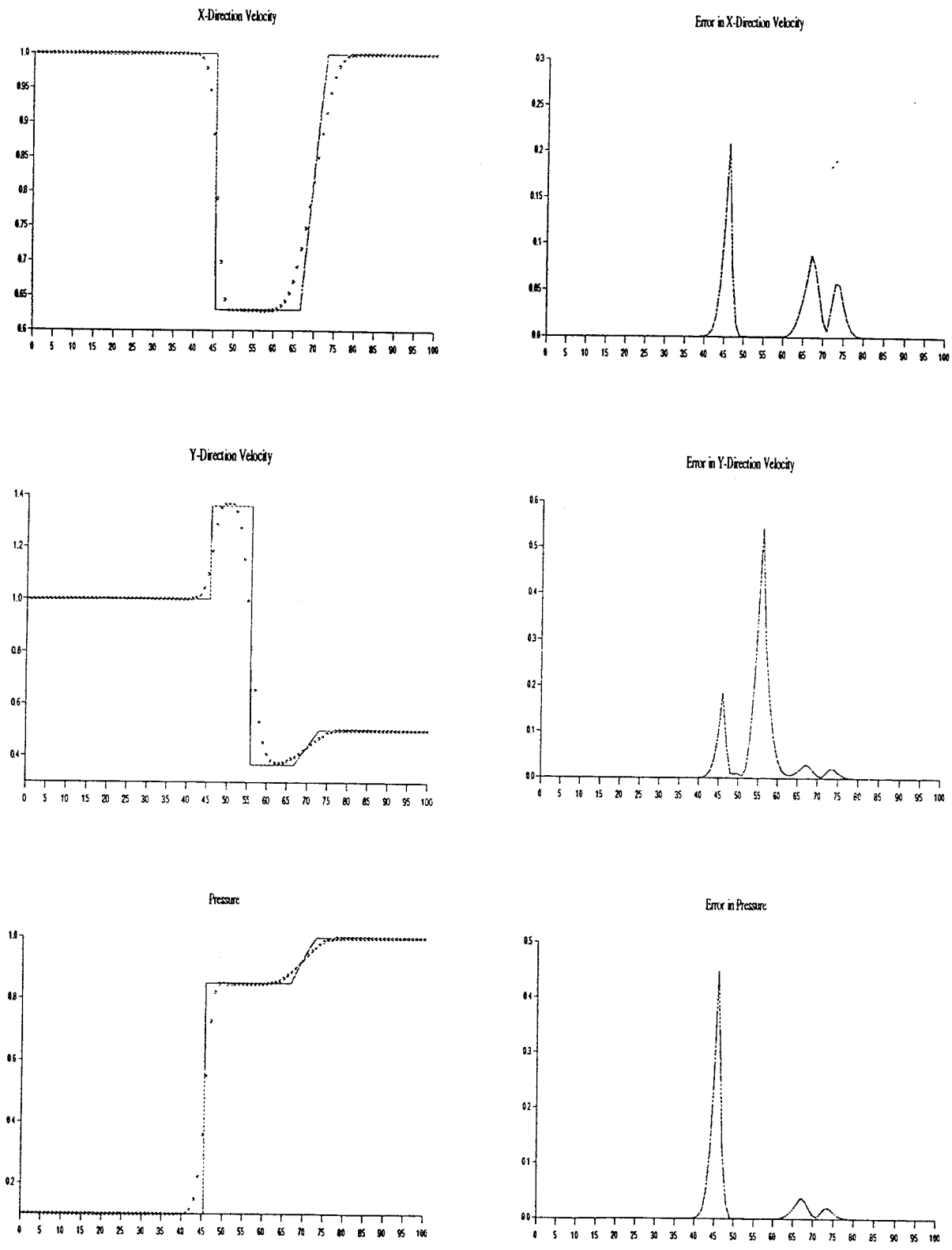

Figure 7: HLLC Riemann Solver